materials proceedings

MDPI

Proceedings

$BiVO_4$-Based Magnetic Heterostructures as Photocatalysts for Degradation of Antibiotics in Water †

Ana C. Estrada *, Filipa Pinto, Cláudia B. Lopes and Tito Trindade

CICECO-Aveiro Institute of Materials, Department of Chemistry, University of Aveiro, 3810-193 Aveiro, Portugal; email1@email.com (F.P.); email2@email.com (C.B.L.); email3@email.com (T.T.)

* Correspondence: ana.estrada@ua.pt

† Presented at the 4th International Online Conference on Nanomaterials, 5–19 May 2023; Available online: https://iocn2023.sciforum.net.

Abstract: Bismuth vanadate ($BiVO_4$) has been investigated as a photocatalyst of great interest due to its ability to harvest photons efficiently in the visible spectral region. In addition, powdered $BiVO_4$ shows high photochemical stability, good dispersibility, and resistance to corrosion in oxidative conditions. Herein, we report the synthesis of monoclinic or tetragonal $BiVO_4$ particles through different methods, as well as the synthesis of hybrids materials through the combination of cobalt ferrite ($CoFe_2O_4$) and $BiVO_4$, and their application in the photodegradation of aqueous solutions of sulfamethoxazole (SMX) under simulated solar radiation. We demonstrate that high-crystallinity single-phase monoclinic $BiVO_4$ was synthesized fast and efficiently using a solid-state method, and their combination with magnetic $CoFe_2O_4$ particles gives rise to a hybrid material that can be easily separated from the reaction medium, by application of an external magnetic field, without the need for further downstream treatments.

Keywords: bismuth vanadate; magnetic photocatalysts; solar-light; water remediation

1. Introduction

According to the World Health Organization, there is a substantial global shortfall in availability of potable water arising from population growth, over-exploitation and industrial contamination and pollution [1]. Although progress has been made in the application of conventional treatment processes, there is urgent need of treatment technologies that produce high quality water using lower energetic input and low costs, as well as not causing harmful effects to humans and environment. The use of solar energy for pollutants' degradation using semiconductor photocatalysts, as well as their recovery and subsequent reuse, is a step forward as an economic and sustainable alternative [2]. Although TiO_2 (Eg 3.2 eV) has been the elective choice for these purposes, there is a great interest to explore other semiconductors whose band gap is located in the visible spectral region [3]. In this way, bismuth vanadate ($BiVO_4$) has been investigated as a photocatalyst of interest due to its ability to harvest photons efficiently in the visible spectral region (Eg 2.4 eV) [4]. In addition, powdered $BiVO_4$ shows high photochemical stability, good dispersibility, and resistance to corrosion in oxidative conditions. However, powdered $BiVO_4$ still presents limitations concerning its separation after photocatalytic reactions and, eventually, regeneration. In this context, the development of nanophotocatalysts with magnetic properties emerges as an advantage regarding the recovery of the photocatalyst and its subsequent reuse. Due to their low cost and availability, magnetic iron oxides, in particular $CoFe_2O_4$ particles, are useful materials to confer the required magnetic properties to the photocatalysts applied to wastewater treatment, [5–7] namely they show fast separation under an external magnetic field due to its high magnetic susceptibility [8].

Citation: Estrada, A.C.; Pinto, F.; Lopes, C.B.; Trindade, T. $BiVO_4$-Based Magnetic Heterostructures as Photocatalysts for Degradation of Antibiotics in Water. *Mater. Proc.* **2023**, *5*, x. https://doi.org/10.3390/xxxxx

Published: 5 May 2023

2. Materials and Methods

2.1. Chemicals

The following chemicals have been used as supplied: bismuth (III) nitrate pentahydrate ($Bi(NO_3)_3.5H_2O$, Sigma-Aldrich, 98%), sodium monovanadate ($NaVO_3$, Sigma-Aldrich, 98%), iron(II) sulfate heptahydrate ($FeSO_4 \bullet 7H_2O$, Panreac, 98%), cobalt(II) chloride hexahydrate ($CoCl_2 \bullet 6H_2O$, Panreac, 99%), potassium hydroxide (KOH, Pronolab, >86%), potassium nitrate (KNO_3, Sigma-Aldrich, >99%), ethanol absolute (Fisher Chemical), and sulfamethoxazole ($C_{10}H_{11}N_3O_3S$, Fluka Chemie). Milli-Q water was obtained from the synergy equipment from Millipore with a 0.22 μm filter.

2.2. Synthesis of Nanomaterials

2.2.1. Synthesis of $BiVO_4$ Nanoparticles

$BiVO_4$ particles were prepared using two different methods, as described below.

- Solid-state synthesis

Pure $BiVO_4$ particles of $BiVO_4$ were synthesized using a solid-state method [9]. In a typical procedure, 1.90 g of $Bi(NO_3)_3 \bullet 5H_2O$ and 0.45 g of NH_4VO_3 were mixed in a mortar and grounded for 30 min to obtain a homogeneous paste. The homogeneous paste was put in a ceramics container and annealed in a tube furnace at 500 °C for 3 h using a heating rate of 2.5 °C/ min. The yellow pristine $BiVO_4$ powder, abbreviated BiV-SS, was collected, washed with water, and dried at room temperature.

- Synthesis under reflux

Typically, 605 mg of $Bi(NO_3)_3.5H_2O$ and 730 mg of EDTA were added to 10 mL of phosphate buffer solution ($[Na_2HPO_4] = [NaH_2PO_4] = 0.1M$), and the mixture was stirred for 10 min. Then, 5 mL of a $NaVO_3$ (305 mg) buffered solution was added to the white milky mixture obtained, which then changed to a yellowish-orange suspension. The pH of this suspension was adjusted to 7 with aqueous NaOH 2M, and the mixture was then stirred at 90 °C for 3 h. The resultant yellow suspension was centrifuged (6000 rpm, 15 min), and the collected material, abbreviated BiV-R, was thoroughly washed with water and ethanol and dried at 60 °C.

2.2.2. Synthesis of Nanoparticles of $CoFe_2O_4$

Magnetic nanoparticles of $CoFe_2O_4$ were synthesized by oxidative hydrolysis of $FeSO_4$. in alkaline conditions [10]. In a typical, 25 mL of deoxygenated water was added to a 250 mL round flask with KOH (1.90 g) and KNO3 (1.52 g). The resulting mixture was heated at 60 °C under a N_2 stream and mechanically stirred at 500 rpm. After salt dissolution, 25 mL of an aqueous solution containing 1.45 g of $CoCl2 \bullet 6H_2O$ and 3.06 g of $FeSO_4 \bullet 7H_2O$ were added dropwise and then the stirring was increased to 700 rpm. After the complete addition of the Fe^{2+} and Co^{2+}ions, the resulting solution was left at 60 °C for 30 min. Then, the round flask was transferred to a hot bath at 90 °C and left under a N_2 stream, without stirring, for 4 h. Finally, the resulting black solid, abbreviated CoFe) was washed several times with deoxygenated water, collected with a laboratorial NdFeB magnet and dried at 40 °C.

2.2.3. Synthesis of BiV-CoFe Hybrid Materials

The hybrid materials composed of both BiVO4 and $CoFe_2O_4$ were synthesized by hydrothermal synthesis. Typically, 5 mg of CoFe was added to 50 mL of an ethanolic suspension containing 250 mg of as-prepared $BiVO_4$ (BiV-SS or BiV-R). The mixture was stirred for 1 h at room temperature, placed in a 100 mL Teflon-lined stainless-steel autoclave sealed and, kept at 120 °C for 12 h. The resulting solid, denominated BiV-SS-CoFe or BiV-R-CoFe, was isolated by filtration, thoroughly washed with water and ethanol, and dried at 40 °C overnight.

2.3. Photocatalytic Studies

The photocatalytic activity of the as-prepared materials was evaluated in the degradation of aqueous solutions of SMX under simulated solar radiation using a Solarbox 1500 (Co.fo.me.gra, Italy). The irradiation device contained an arc xenon lamp (1500 W) and outdoor UV filters that limited the transmission of light with wavelengths below 290 nm. The irradiance of the lamp was set to 55 W m^{-2} (290–400 nm) and was kept constant during all the experiments. To monitor the irradiance level and temperature, a multimeter (Co.fo.me.gra, Italy), equipped with a UV (290–400 nm) large band sensor and a black standard temperature sensor, was used. In a typical photocatalytic run, the 10 mg of material was dispersed in 30 mL of aqueous solution of SMX (5 mg/L) and before the irradiation the reaction was stirred in the dark for 30 min, to ensure the adsorption/ desorption equilibrium of SMX molecules over the materials. The concentration of SMX was analysed by HPLC-DAD at 265 nm using a column Kromasil 100-5-C18 (250 mm in length and 4.6 mm of i.d.). The column was maintained at 30 ºC and the mobile phase consisted of acetic acid 1M (70%) and methanol (30%) with a flow rate of 0.8 mL/min. The SMX adsorption capacity of all-prepared materials was evaluated using the same experimental procedure but keeping the mixture in the dark, under vigorous stirring. The photodegradation rate was calculated according to Equation (1), where C_t and C_0 are the concentration of RhB or SMX at time t and t = 0, respectively.

$$R = \frac{C_0 - C_t}{C_0} \times 100\% \quad (1)$$

3. Results

3.1. Characterization of Materials

The powder XRD patterns of BiV-SS, BiV-R, CoFe particles, as well as the hybrid materials, BiV-SS-CoFe and BiV-R-CoFe, are shown in Figure 1A,B.

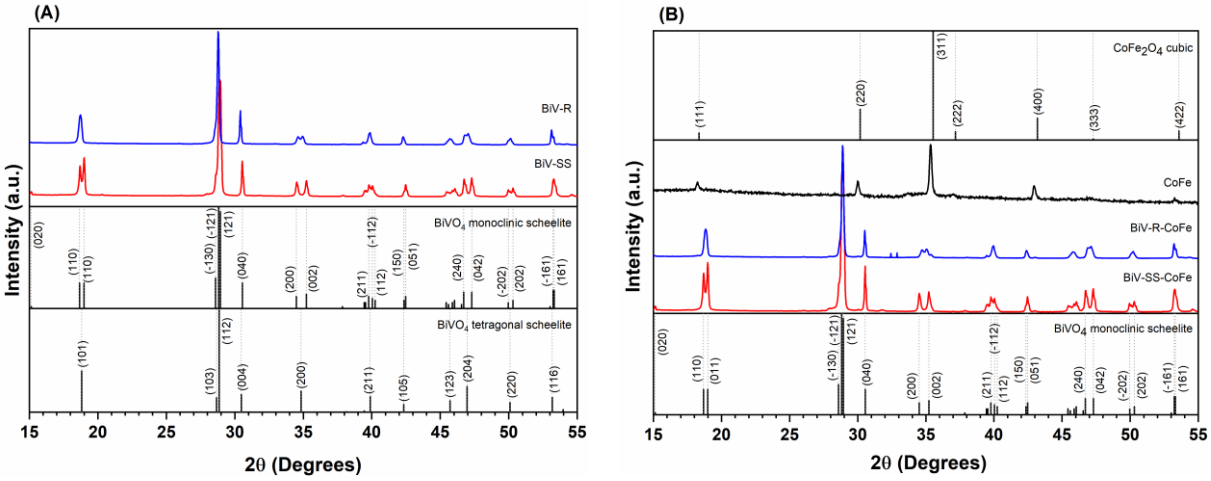

Figure 1. Powder XRD patterns of (**A**) BiV-SS and BiV-R and; (**B**) CoFe, BiV-SS-CoFe and BiV-R-CoFe. The vertical lines correspond to the standard diffraction peaks attributed to the $BiVO_4$ monoclinic scheelite phase (ICDDPDF N.º 00-014-0688), $BiVO_4$ tetragonal scheelite phase (ICDDPDF N.º 04-010-5710) and $CoFe_2O_4$ cubic phase (ICDDPDF N.º 01-086-4438).

It is well-known that $BiVO_4$ exists in three natural polymorphs—pucherite, dreyerite and clinobisvanite. The monoclinic clinobisvanite (or monoclinic scheelite, m-s) and tetragonal dreyerite (or tetragonal zircon, t-z) are also obtained synthetically, whereas the orthorhombic polymorph pucherite exists only naturally [11]. In addition to these polymorphs, synthetic $BiVO_4$ is also known to crystallize in the tetragonal scheelite structure, t-s, which shows a similar structure to m-s $BiVO_4$, with tetrahedrally coordinated V(V)

and eight-fold coordinated Bi(III), but differing in the Bi-O polyhedron which is more distorted by the $6s^2$ lone electron pair resulting in the loss of four-fold symmetry [12–14]. The t-s $BiVO_4$ exhibits single reflections at $2\theta = 18.5°$, 35° and 46° related to the (101), (200) and (204) reflections (ICDDPDF No. 04-010-5710), while, the m-s crystalline phase presents splitting of peaks at 18.5°, 35° and 46° corresponding to the crystalline planes [(101), (011)], [(200), (002)] and [(240), (042)], respectively, and a less intense peak at 15°, (ICDDPDF No. 00-014-0688). Hence, it was found that the solid-state method leads to the formation of m-s $BiVO_4$, while the synthesis by reflux seems to give rise to a mixture of the two phases, m-s and t-s $BiVO_4$ (Figure 1A). Regarding the hybrid materials, it was found that the coupling of CoFe nanoparticles preserves the initial crystalline structure of $BiVO_4$, continuing to observe the m-s $BiVO_4$ in the hybrid prepared from BiV-SS, obtained by the solid-state method (Figure 1B). Although the presence of the magnetic phase in the hybrid materials is not evident in the XRD pattern of hybrid materials, it was possible to infer their magnetic character when they are exposed to an external magnetic field (Figure 2A).

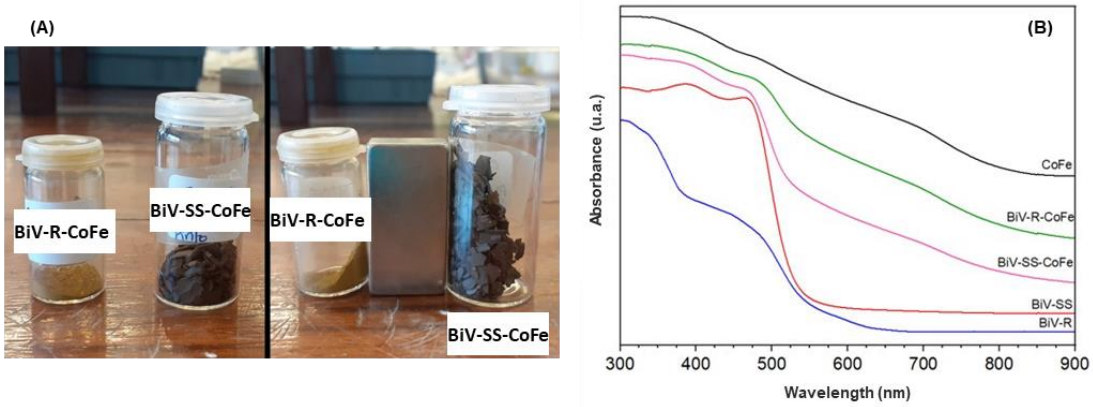

Figure 2. (**A**) BiV-R-CoFe and BiV-SS-CoFe hybrid materials before and 2 min after exposure to a magnet and; (**B**) UV-Vis spectra of hybrid materials and respective individual components.

The UV-VIS diffuse reflectance spectra of the hybrid sample and $BiVO_4$ particles are shown in Figure 2B. The spectrum of pristine $BiVO_4$ shows a strong absorption around 500 nm, which corresponds to the band gap transition involving the Bi 6s and V 3d levels, in accordance with the reported data [15]. The coupling of $BiVO_4$ particles with CoFe slightly extends the wavelength absorption range for photon harvesting in the hybrid photocatalyst.

3.2. Photocatalytic Studies

The photocatalytic performance of hybrid materials, as well as their single components, was evaluated through the degradation, under visible-light irradiation, of SMX. Figure 3 shows the adsorption behaviour of materials, under dark conditions. It was found that the pseudo-first-order model shows a more suitable R^2 than the pseudo-second-order, indicating that the pseudo-first-order was indeed followed in the processes (Table 1). At 15 min of contact time, the mass of SMX adsorbed on BiV-R and BiV-R-CoFe was 0.45 and 0.2 mg/g, respectively, and 0.8 and 0.4 mg/g of SMX for BiV-SS and BiV-SS-CoFe, respectively, after 30 min. Thus, we can assume that both the hybrids and the individual components have low adsorption capacity for SMX.

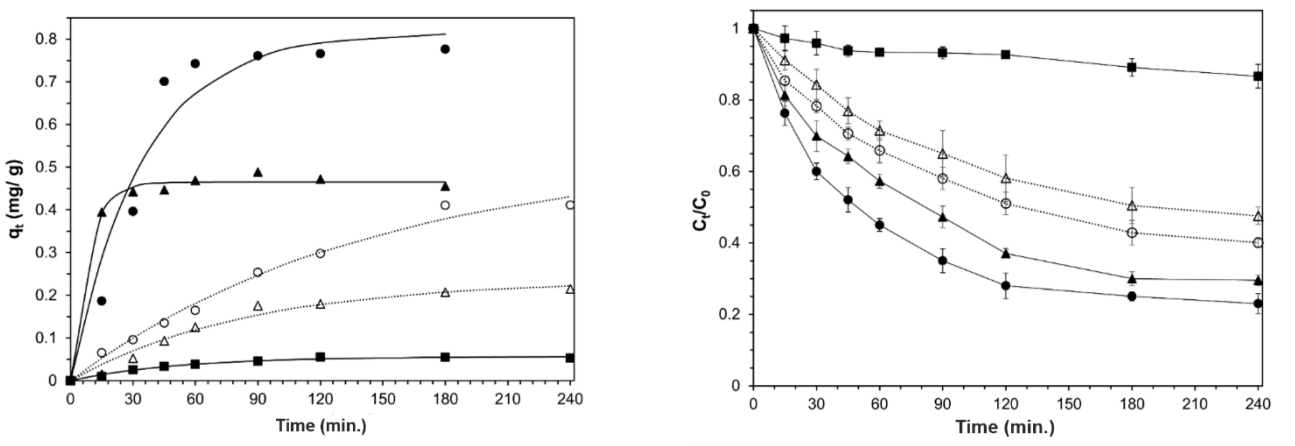

(**A**) (**B**)

Figure 3. (**A**) Nonlinear pseudo-first-order kinetic plot of SMX (5 mg/L) adsorption at room temperature and pH 5 using 10 mg of material and; (**B**) Kinetics curves of SMX (5 mg/L) photodegradation. ●BiV-SS; ▲BiV-R; ○BiV-R; △BiV-R-CoFe; and ■CoFe.

Table 1. Parameters obtained by modelling the pseudo-first-order and pseudo-second-order nonlinear isotherms of SMX adsorption onto hybrid materials or their individual components (C_0 = 5 mg/L and 10 mg of adsorbent).

Sample	Pseudo-First-Order		Pseudo-Second-Order	
	q_1 (mg/g)	R^2	q_2 (mg/g)	R^2
BiV-SS	0.82	0.94	1.01	0.91
BiV-R	0.46	0.99	0.48	0.99
BiV-SS-CoFe	0.53	0.99	0.82	0.98
BiV-R-CoFe	0.24	0.97	0.33	0.95
CoFe	0.06	0.98	0.07	0.96

Figure 2B shows the concentration of SMX as a function of light irradiation time in the presence of hybrid materials, as well as in the presence of individual components. The degradation SMX in the presence of CoFe was very low; less than 10% of SMX were removed after 240 min of irradiation. In the presence of pure BiV-SS or BiV-R, it was attained 75% or 70% of SMX removal, respectively. In the presence of hybrid materials, moderate degradation values of SMX (60% for BiV-SS-CoFe and 50% for BiV-R-CoFe) were observed, after 240 min of irradiation. Although slightly lower, the advantages (recovery and reuse) of the hybrid materials can compensate the slight lower degradation values obtained in comparison with their individual components. Photocatalytic degradation of SMX in the presence of as-prepared materials followed the pseudo-first-order kinetic model, following the equation $C/C_0 = e^{-kt}$, and the reaction rate constant (k) was determined from the slope of linear $-Ln(C/C_0)$ as a function of the time (t) plot, where C_0 and C are the initial and remaining concentrations of SMX, at different irradiation times, respectively. The k values for the photocatalytic degradation of SMX were 1.2 × 10^{-2}, 0.87 × 10^{-2}, 0.62 × 10^{-2} and 0.42× 10^{-2} min^{-1} for BiV-SS, BiV-R, BiV-SS-CoFe and BiV-R-CoFe, respectively.

4. Conclusions

The photocatalytic activity of the hybrid materials, BiV-SS-CoFe and BiV-R-CoFe, was studied for photodegradation of SMX under simulated solar radiation and compared with corresponding individual components. It was found that the best photocatalyst was BiV-SS with 75% of SMX photodegradation, followed by BiV-R with 70%. When comparing the photocatalytic activity of respective hybrid materials, it was found moderate values of SMX photodegradation, 60% in the case of BiV-SS-CoFe and 50% for BiV-R-CoFe.

Although slightly lower, the advantages of recovery and reuse of the hybrid materials can compensate for the lower degradation values obtained in comparison with individual components.

Supplementary Materials: The following are available online at www.mdpi.com/xxx/s1, Figure S1: title, Table S1: title, Video S1: title.

Acknowledgments: This work was developed within the scope of the project CICECO-Aveiro Institute of Materials, UIDB/50011/2020, UIDP/50011/2020 & LA/P/0006/2020, financed by national funds through the FCT/MCTES (PIDDAC). Ana C. Estrada thanks the costs of her research contract resulting from the FCT hiring funded by National funds (OE), through FCT, I.P., in the scope of the framework contract foreseen in 4, 5, and 6 of article 23 of the Decree-Law 57/2016, of 29 August, changed by the law 57/2017, of 19 July. Claudia B. Lopes also acknowledge her Researcher Contract CEECIND/03739/202.

Conflicts of Interest: The authors declare no conflict of interest.

References

1. UNICEF; WHO. *Progress on Sanitation and Drinking Water. 2015 Update and MDG Assessment*; World Health Organization: Geneva, Switzerland, 2015.
2. Lopes, J.L.; Martins, M.J.; Nogueira1, H.I.S.; Estrada, A.C.; Trindade, T. Carbon-based heterogeneous photocatalysts for water cleaning technologies: A review. *Environ. Chem. Lett.* **2021**, *19*, 643–668.
3. Gaya, U.I. *Heterogeneous Photocatalysis Using Inorganic Semiconductor Solids*, 2014th ed., Springer: Berlin/Heidelberg, Germany, 2014.
4. Kudo, A.; Miseki, Y. Heterogeneous photocatalyst materials for water splitting. *Chem. Soc. Rev*. **2009**, *38*, 253–278.
5. Liu, C.; Zhang, X.; Li, W.; Yu, Y.; Liu, M.; Wang, L.; Li, C.; Zhang, X.; Liu, X.; Lin, X. Leaf-like $BiVO_4$ nanostructure decorated by nitrogen-doped carbon quantum dots: Binary heterostructure photocatalyst for enhanced photocatalytic performance. *Mater. Res. Bull*. **2020**, *122*, 110640.
6. Liu, S.Q. Magnetic semiconductor nano-photocatalysts for the degradation of organic pollutants. *Environ. Chem. Lett*. **2012**, *10*, 209–216.
7. Tahar, L.B.; Oueslati, M.H.; Abualreish, M.J.A. Synthesis of magnetite derivatives nanoparticles and their application for the removal of chromium (VI) from aqueous solutions. *J. Colloid Interface Sci*. **2018**, *512*, 115–126.
8. Wu, W.; Wu, Z.; Yu, T.; Jiang, C.; Kim, W.S. Recent progress on magnetic iron oxide nanoparticles: Synthesis, surface functional strategies and biomedical applications. *Sci. Technol. Adv. Mater*. **2015**, *16*, 023501.
9. Ma, J.-S.; Lin, L.-Y.; Chen, Y.-S. Facile solid-state synthesis for producing molybdenum and tungsten co-doped monoclinic $BiVO_4$ as the photocatalyst for photoelectrochemical water oxidation. *Int. J. Hydrog. Energy* **2019**, *44*, 7905–7914.
10. Oliveira-Silva, R.; Da Costa, J.P.; Vitorino, R.; Daniel-Da-Silva, A.L. Magnetic chelating nanoprobes for enrichment and selective recovery of metalloproteases from human saliva. *J. Mater. Chem. B* **2015**, *3*, 238–249.
11. Lu, Y.; Shang, H.; Shi, F.; Chao, C.; Zhang, X.; Zhang, B. Preparation and efficient visible light-induced photocatalytic activity of m-$BiVO_4$ with different morphologies. *J. Phys. Chem. Solids* **2015**, *85*, 44–50.
12. Ke, D.; Peng, T.; Ma, L.; Cai, P.; Dai, K. Effects of hydrothermal temperature on the microstructures of $BiVO_4$ and its photocatalytic O_2 evolution activity under visible light. *Inorg. Chem*. **2009**, *48*, 4685–4691.
13. Nagabhushana, G.P.; Tavakoli, A.H.; Navrotsky, A. Energetics of bismuth vanadate. *J. Solid State Chem*. **2015**, *225*, 187–192.
14. Tokunaga, S.; Kato, H.; Kudo, A. Selective preparation of monoclinic and tetragonal $BiVO_4$ with scheelite structure and their photocatalytic properties. *Chem. Mater*. **2001**, *13*, 4624–4628.
15. Lardhi, S.; Cavallo, L.; Harb, M. Determination of the intrinsic defect at the origin of poor H_2 evolution performance of the monoclinic $BiVO_4$ photocatalyst using Density Functional Theory. *J. Phys. Chem. C* **2018**, *122*, 18204–18211.